An optimized prediction of FRP bars in concrete bond strength employing soft computing techniques

Rwayda Kh S. Al-Hamd [a],[*], Asad S. Albostami [b],[c], Saif Alzabeebee [d], Baidaa Al-Bander [e]

[a] School of Applied Sciences, Abertay University, Dundee, UK
[b] Civil Engineering Department, Faculty of Engineering, University of Petra, Amman, Jordan
[c] School of Engineering & Construction, Oryx Universal College in Partnership with Liverpool John Moores, Doha, Qatar
[d] Department of Roads and Transport Engineering, College of Engineering, University of Al-Qadisiyah, Al Diwaniyah, Al-Qadisiyah, Iraq
[e] School of Computing, Keele University, Keele, Newcastle, ST5 5BG, UK

ABSTRACT

The precise estimation of the bonding strength between concrete and fiber-reinforced polymer (FRP) bars holds significant importance for reinforced concrete structures. This study introduces a new methodology that utilizes soft computing methods to enhance the prediction of FRP bars' bonding strength. A significant compilation of experimental bond strength tests is assembled, covering various variables. Significant variables that affect bonding strength are found in the study of this database. The prediction process is optimized using soft computing methods, particularly Gene Expression Programming (GEP) and the Multi-Objective Genetic Algorithm Evolutionary Polynomial Regression (MOGA-EPR).

The proposed soft computing approaches accommodate complex relationships and optimize prediction accuracy depending on the input variables. Results demonstrate its effectiveness in predicting bond strength and comparing it with existing codes and other models from the literature. The results have shown that the MOGA-EPR and the GEP models have high R^2 values between 0.91 and 0.94. The proposed new models enhance the reliability and efficiency of designing and assessing FRP-reinforced concrete.

1. Introduction and background

The bond behavior between fiber-reinforced polymer (FRP) bars and concrete is a crucial aspect of the design and durability of reinforced concrete structures. FRP bars offer numerous advantages over traditional steel reinforcement, such as high corrosion resistance, lightweight properties, and good fatigue behavior. As a result, there has been increasing interest in utilizing FRP bars as internal reinforcement in concrete structures [1–3]. The FRP behave slightly differently from the normal steel reinforcement bars; therefore, it is important to investigate [4–7].

Understanding the bond strength between FRP bars and concrete is essential for ensuring the structural integrity and performance of FRP-reinforced concrete elements. The bond strength refers to the ability of the interface between the FRP bar and concrete to transmit stress effectively. It depends on various factors, including surface roughness, bar diameter, concrete compressive strength,

---

epoxy adhesive properties, curing conditions, and environmental factors [1].

Accurate prediction of the bond strength is crucial for designing and assessing FRP-reinforced concrete structures. Traditional empirical equations have limitations in capturing the complex and nonlinear behavior of the bond interface and may not account for all relevant parameters. To overcome these limitations, researchers have turned to advanced computational techniques, particularly soft computing approaches, which can handle complex relationships and optimize prediction accuracy [1].

Over the past twenty years, there has been a growing trend in the utilization of Fiber Reinforced Polymer (FRP) bars in reinforced concrete constructions, gradually replacing traditional steel reinforcement, particularly in regions with challenging environmental conditions. Nepomuceno et al. [8] present a review of literature concerning the adherence characteristics of FRP bars to concrete, encompassing investigations into their immediate and prolonged (durability) attributes. Additionally, this study involves the compilation of experimental data from existing literature, comprising outcomes from a total of 1002 pullout tests, aimed to explain the key factors influencing the bond between FRP bars and concrete. Analysis of this dataset led to the conclusion that FRP bars demonstrate commendable performance as reinforcements in concrete structures. Furthermore, the assembled data facilitated the formulation of long-term predictions regarding the bond (durability) between FRP bars and concrete, considering the nature of the exposure environment. On the other hand, Li et al. [9] propose a novel approach to address the weakening bonding performance of fiber-reinforced plastic (FRP) rebars compared to mild steel, caused by corrosion avoidance. They introduce a particle swarm optimization-based extreme learning machine model, utilizing 222 samples and six input variables to accurately estimate FRP bar bond strength. The model incorporates factors such as bar position, surface condition, diameter, concrete strength, and ratios related to bar and concrete thickness. Results demonstrate the model's effectiveness ($R^2 = 0.945$) compared to the original model ($R^2 = 0.926$), offering a valuable tool for FRP bar bond analysis.

Pei & Wei [10] propose a hybrid model integrating ant colony optimization and fuzzy c-means clustering into an adaptive neuro-fuzzy inference system to predict bond strength between FRP sheets and concrete. Their model outperforms existing empirical models, exhibiting higher accuracy and efficiency. Shahri & Mousavi [11] addresses the bond between concrete and glass fiber reinforced polymer (GFRP) rebars using soft computing techniques. They collect data from hinged beam tests, employing Kriging, multivariate adaptive regression splines, and nonlinear regression to predict bond resistance. Jahangir et al. [12] presents new models calibrated through soft computing to accurately predict bond strength between textile-reinforced mortars (TRMs) and concrete, overcoming inaccuracies of existing models and providing valuable insights into TRM-concrete bond strength estimation.

Even yet, conventional regression analysis was used to construct the analytic correlations described here. The current Eurocode method applies a simplified approximation based on the tensile strength design of concrete to simulate "excellent" or "poor" bond circumstances. Contrarily, structural engineers are beginning to see the significance of recent developments in artificial intelligence (AI) and machine learning (ML), which may improve design advice [13]. When compared to the current methodologies, one method employed in the civil engineering disciplines of hydraulic geotechnical and structural engineering offers improved accuracy [14–27]. Using a progressive regression analysis technique to bond strength is covered in a paper by Al-Hamd et al. [28]. This method generates a very precise estimate of binding strength using the multi-objective evolutionary polynomial regression analysis (MOGA-EPR).

GEP has various advantages, such as its ability to handle a variety of optimization problems, generate programs automatically, incorporate domain-specific knowledge flexibly, and effectively capture nonlinear relationships. A model has been developed to estimate bond strength between fiber-reinforced polymer (FRP) bars and concrete using Gene Expression Programming (GEP). The model uses input parameters including the width of FRP, the width of concrete, the thickness of FRP, the elastic modulus of FRP, concrete compressive strength, and bond length. The GEP model was able to derive a new relationship for predicting the bond strength of FRP-to-concrete composite joints by dividing the collected data into trained and tested sets. The results demonstrate the effectiveness of the GEP model in predicting bond strength values and its derived relationship outperforms other existing models in terms of convenience and accuracy. Among the models presented by other researchers, the model proposed by Ref. [29] demonstrates better accuracy, while the model offered by Ref. [30] exhibits the lowest accuracy [31].

The utilization of GEP provides a powerful tool for predicting bond strength in FRP-to-concrete composite structures. By incorporating multiple input parameters and employing an advanced computational technique, the GEP model enhances the understanding and estimation of bond strength. This contributes to the efficient design and evaluation of FRP-reinforced concrete elements, ultimately advancing the field of structural engineering and promoting the use of FRP as a viable reinforcement option.

The current prediction of bond strength relies exclusively on conventional rebars, neglecting the influence of FRP. This omission makes it more difficult to evaluate the overall structural integrity because FRP has different characteristics that can have an impact on bond strength. This could result in inaccurate estimates of the bond strength. Therefore, this work addresses the inclusion of the effect of the FRP on the bond strength.

Improving the understanding and prediction of bond strength between FRP bars and concrete contributes to the effective design, assessment, and utilization of FRP-reinforced concrete structures. It enables engineers to make informed decisions regarding material selection, structural performance, and durability. By leveraging soft computing techniques, this research aims to enhance the reliability and efficiency of FRP-reinforced concrete applications, ultimately advancing the field of structural engineering [31].

This study aims to explore and optimize the prediction of bond strength between FRP bars and concrete using soft computing techniques. By compiling and analyzing a comprehensive database of experimental bond strength tests, significant parameters influencing the bond behavior will be identified. Multi-Objective Genetic Algorithm Evolutionary Polynomial Regression (MOGA-EPR) and Gene Expression Programming (GEP) will be developed to predict the bond strength and optimize model parameters accurately.

2. Current methods and codes

The current literature highlights the parameters that impact the bond strength (τ). The key parameter is the compressive strength of the concrete (f_c'). The secondary parameters that play are role are the bar diameter (d_b), bar embedment length to bar diameter ratio ($\frac{l_d}{d_b}$), and concrete cover-to-bar diameter ratio ($\frac{c}{d_b}$). According to a study conducted by Ref. [32], in 2019, it has been proposed that the bond strength can be predicted by considering two factors: the surface of the bar (referred to as Surf) and the position of the bar (referred to as Pos). In their research, they assumed that a value of 1 or 2 for the bar position variable represents the top or bottom location of the FRP bars in the beam bond test. Additionally, the values 1, 2, and 3 for the bar surface variable correspond to helical lugged surfaces, spiral-wrapped surfaces, and sand-coated surfaces of FRP bars.

Table 1 presents Equations 1 to 10, which depict the current method used for estimating the bond strength:

3. Methodology

This study examines the ability to predict the bond strength of FRP bars in concrete by employing the MOGA-EPR and GEP approaches. A collection of experimental data gathered from recent literature acts as the basis for training and assessing the bond strength. Subsequently, the outcomes of the MOGA-EPR and two GEP models will be contrasted with various analytical models and methods currently in existence.

The flowchart represented in Fig. 1 provides an overview of the methodology and process employed in this study. It begins with data collection, followed by statistical analysis, data grouping, model development, calculation of statistical indicators, analysis of the results, assessment, and the examination of sensitivity studies. The sensitivity analysis investigates the impact of factors such as the compressive strength of concrete (f_c'), the position and surface of the bars on the bond strength (τ).

3.1. Data analysis

The models in this work were created using an experimental database of 223 test results for the bond strength of FRP concrete that was gathered from the literature by Ref. [32]. The data was selected to reflect on the variables that affect the bond strength based on the literature and these variables are explained in section 3.3.

Table 2 displays the statistical metrics derived from the gathered data, revealing the minimum, maximum, mean, and standard deviation values of both input parameters and the experimental bond strength between FRP bars and concrete datasets. These indicators are crucial for understanding data distribution, assessing quality, guiding model training, selecting features, evaluating model performance, and analyzing uncertainties. They provide insights into dataset characteristics, aid in model development, and ensure robustness in predictive analyses.

3.2. Data grouping

In order to predict bond strength (τ), this study compared the effectiveness of two Gene Expression Programming (GEP) models to a Multi-Objective Genetic Algorithm Evolutionary Polynomial Regression (MOGA-EPR) model. To ensure accuracy, the acquired data was split into two sets: 80 % for training the models and 20 % for testing. Tables 3 and 4 give the statistical metrics relevant to the

Table 1
Equations for existing methods and codes.

| Reference	Bond strength of FRP bars in concrete (τ) equation	Equation #
Wang et al., 2021 Model I [33]	$\tau_{max} = 0.09 f_c' - 0.655$	Eq. (1)
Wang et al., 2021 Model II [33]	$\tau_{max} = -0.054 f_c' + 0.7\sqrt{f_c'} - 1.193$	Eq. (2)
MGGP, 2019 [32]	$\tau_{max} = 0.0665 f_c' - 0.189 d_b + 0.0406 \frac{l_d}{d_b} + 2.26 \ln\left(\frac{c}{d_b} \times \frac{l_d}{d_b}\right) - 0.0665\left(\frac{c}{d_b}\right)^3 -$ $4.16 \ln\left(2\text{Surf} + \frac{l_d}{d_b} + \left(f_{jc} \times \frac{l_d}{d_b}\right)\right) + 0.00558 \ln\left(\frac{l_d}{d_b}\right) + 0.0175\left(\text{Pos} \times \frac{l_d}{d_b}\right) -$ $0.00108(f_c')^2 + 39.8$	Eq. (3)
Diab et al., 2014 [34]	$\tau_{max} = 0.08305\sqrt{f_c'}\left[22.8 + 0.208\left(\frac{c}{d_b}\right) + 38.212\left(\frac{d_b}{l_d}\right)\right]$	Eq. (4)
Aslani & Nejadi, 2012 [35]	$\tau_{max} = \left[0.7\left(\frac{c}{d_b}\right)^{0.6} + 4\left(\frac{d_b}{l_d}\right)\right](f_c')^{0.23}$	Eq. (5)
ACI, 2006 [32]	$\tau_{max} = f_c'\left(0.332 + 0.025 \frac{c}{d_b} + 8.3 \frac{d_b}{l_d}\right)$	Eq. (6)
CEB-FIP I [36]	$\tau_{max} = 2.5\sqrt{f_c'}$	Eq. (7)
CEB-FIP II [36]	$\tau_{max} = 7\left(\sqrt{\frac{f_c'}{25}}\right)^{0.25}$	Eq. (8)
CEB-FIP III [36]	$\tau_{max} = 13.5\sqrt{\frac{f_c'}{30}}$	Eq. (9)
Orangun et al., 1977 [37]	$\tau_{max} = 0.083045\sqrt{f_c'}\left[1.2 + 3\left(\frac{c}{d_b}\right) + 50\left(\frac{d_b}{l_d}\right)\right]$	Eq. (10)
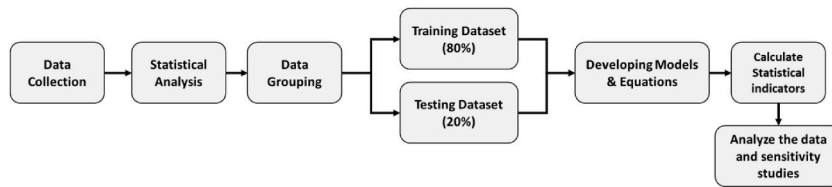
Fig. 1. Flowchart illustrating the methodology process described in the paper.

Table 2
Statistical indicators for the collected datasets.

	Position	Surface	d_b	$f'c$	c/d_b	l_d/d_b	τ _Experiment_
Min.	1.00	1.00	6.35	23.43	1.68	3.56	0.76
Max.	2.00	3.00	28.58	55.06	9.34	115.79	21.00
Average	1.87	1.72	14.65	40.04	3.58	30.14	6.79
STDEV	0.34	0.76	4.89	6.72	1.82	23.01	4.15

Table 3
Statistical indicators for the training dataset.

	Position	Surface	d_b	$f'c$	c/d_b	l_d/d_b	τ _Experiment_
Min.	1.00	1.00	6.35	23.43	1.68	3.56	0.97
Max.	2.00	3.00	28.58	55.06	9.34	115.79	21.00
Average	1.87	1.72	14.61	39.98	3.54	29.55	7.02
STDEV	0.34	0.76	4.84	6.80	1.81	22.91	4.31

Table 4
Statistical indicators of the testing dataset.

	Position	Surface	d_b	$f'c$	c/d_b	l_d/d_b	τ _Experiment_
Min.	1.00	1.00	6.35	27.25	1.68	5.00	0.76
Max.	2.00	3.00	28.58	51.98	9.34	97.24	19.35
Average	1.89	1.71	14.83	40.26	3.78	32.46	5.89
STDEV	0.32	0.73	5.12	6.51	1.86	23.52	3.37

training and testing datasets and Fig. 2 for the data frequency.

Fig. 3 shows a heatmap to show the correlation matrix. In this matrix correlation coefficient close to 1 indicates a strong positive correlation and close to −1 indicates a negative correlation. Meanwhile, the correlation coefficient close to 0.0 suggests little to no linear relationship between the variables.

Fig. 4 shows a scatter plot that is a graphical representation of the relationship between two input variables and the output. These plots demonstrate the impact of each of the input variable changes in relation to the output.

3.3. Developing the models

This study aimed to predict the Bond Strength (τ) of FRB reinforcement bars in MPa by constructing models through two approaches: MOGA-EPR and GEP. These models were developed using six input variables, namely the compressive strength of the concrete (f'_c) in MPa, the bar diameter (d_b) in mm, bar embedment length to bar diameter ratio ($\frac{l_d}{d_b}$), concrete cover-to-bar diameter ratio ($\frac{c}{d_b}$), the surface characteristics of the bar (Surf), and the position of the bar (Pos). According to the literature [28] the concrete strength, represented by the compressive strength (f'_c) is foundational as with higher strength correlating to stronger bond since the concrete will have a better bonding surface. Bar diameter (d_b) directly influences bond strength as it provides a higher contact surface area to bond, and the ratio of embedment length to bar diameter ($\frac{l_d}{d_b}$) captures the impact of embedded length. The concrete cover-to-bar diameter ratio ($\frac{c}{d_b}$) reflects the protective layer, while surface characteristics (Surf) and bar position (Pos) account for mechanical interlocking and positional differences, respectively. By accounting for the (Surf) and the (Pos) in the prediction equations, engineers and researchers can ensure more reliable and precise estimations of bond strength, leading to safer and more robust FRP-reinforced concrete structures. The process of creating these models is described as follows:

#### 3.3.1. Multi-objective evolutionary polynomial regression (MOGA- EPR)

The computational technique known as Multi-objective Evolutionary Polynomial Regression Analysis (MOGA-EPR) uses input data to take advantage of input issues and identify solutions. Using a genetic algorithm (GA), regression analysis is utilized to generate a mathematical correlation. This correlation demonstrates the relationship between the physical input variables. By introducing several
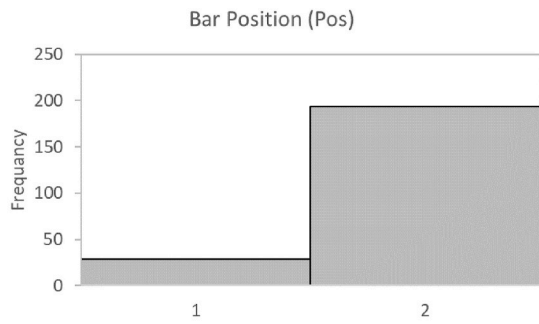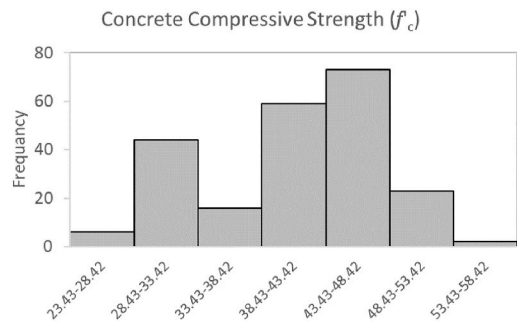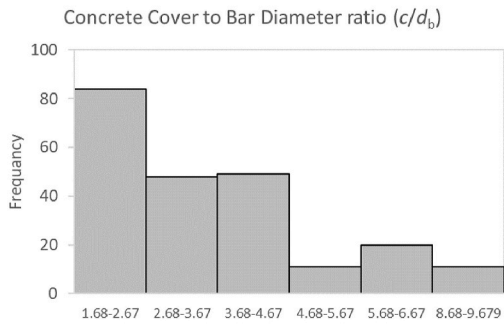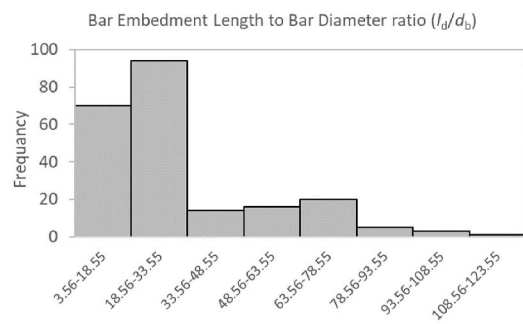
(a) Bar Position
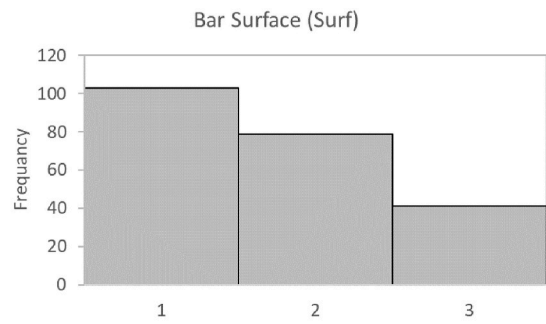
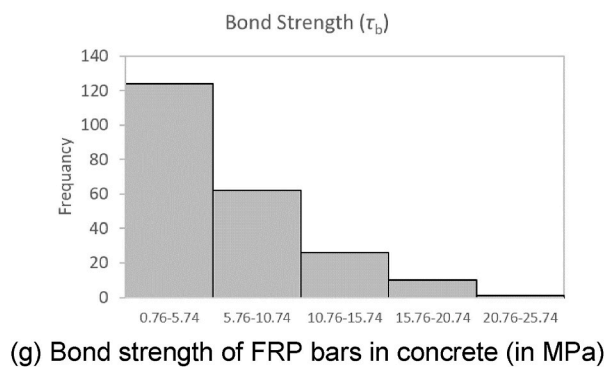**(b) Bar Surface**
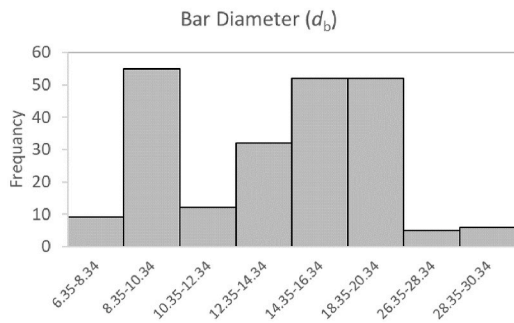
(c) Bar Diameter (in mm)

(d) Concrete Compressive Strength (in MPa)

(e) Concrete cover-to-bar diameter ratio

(f) Bar embedment length to bar diameter ratio

(g) Bond strength of FRP bars in concrete (in MPa)

Fig. 2. Frequency of the collected data parameters.

Fig. 3. Heatmap for the variable.

targets, the EPR-GA, MOGA reduce the correlation's complexity while improving precision. This regression approach differs from standard regression in that it uses a search algorithm to automatically discover the optimal correlation and avoids the overfitting problem that classic regression methods frequently experience. The structure of the correlation, the range of exponents, and the number of terms must all be known by the user before using the EPR-MOGA. You may read more about the EPR-MOGA in detail in Ref. [28,25–27,38–41]. Table 5 shows the equation obtained by MOGA-EPR (Equation (11)).

The search for the optimal values of parameters and exponents is a crucial step in developing accurate models. In this process, EPR-MOGA is utilized to strike a balance between competing objectives, as explained by Ref. [42]. By doing so, this allows the selection of coefficients that meet the expected performance as required in Equation (11).

3.3.2. Gene Expression Programming (GEP)

Studies by Ref. [43,44] show that the GEP method, which is an enhanced version of Genetic Programming (GP) proposed by Ref. [45], is effective at simulating complicated and nonlinear processes. The GEP method is used in this work to forecast the bond strength of FRP bars in concrete. According to Ref. [45], GEP defines people as linear chromosomes with defined lengths that can be converted into tree structures. Valid and accurate solution structures can be produced by applying genetic operators like mutation and recombination to the linear structure of chromosomes.

In this study, GEP analysis was performed using the GeneXproTools software as described by Ref. [46]. To generate the initial population of solutions, a variety of functions including basic arithmetic, trigonometric, logarithmic, and polynomial functions, as well as constant values and independent problem variables known as terminals, were incorporated. These chromosomes were represented as tree expressions. The fitness of each member of the population was assessed using the fitting function introduced by Ref. [47].

To create an optimal solution for a specific problem, the GEP model uses an iterative approach, adhering to the guidelines set out by Ref. [45]. Starting with the starting population, chromosomes are generated at random and expressed as tree expressions. Each chromosome's compatibility and suitability are then assessed. The program ends and the existing population serves as the solution when the desired conditions are satisfied. The population's most promising people are kept, while the others are chosen based on how well they perform. The chosen population is then improved upon and altered, leading to the birth of descendants with novel traits. These new children go through the same developmental cycle, and the cycle is repeated until a satisfactory solution is attained for a certain number of generations.

Table 6 displays the main configuration parameters and modifications of the GEP model, which are analogous to those used in the MOGA-EPR model. Additionally, Table 7 presents Equations 12 and 13 for the two GEP models.
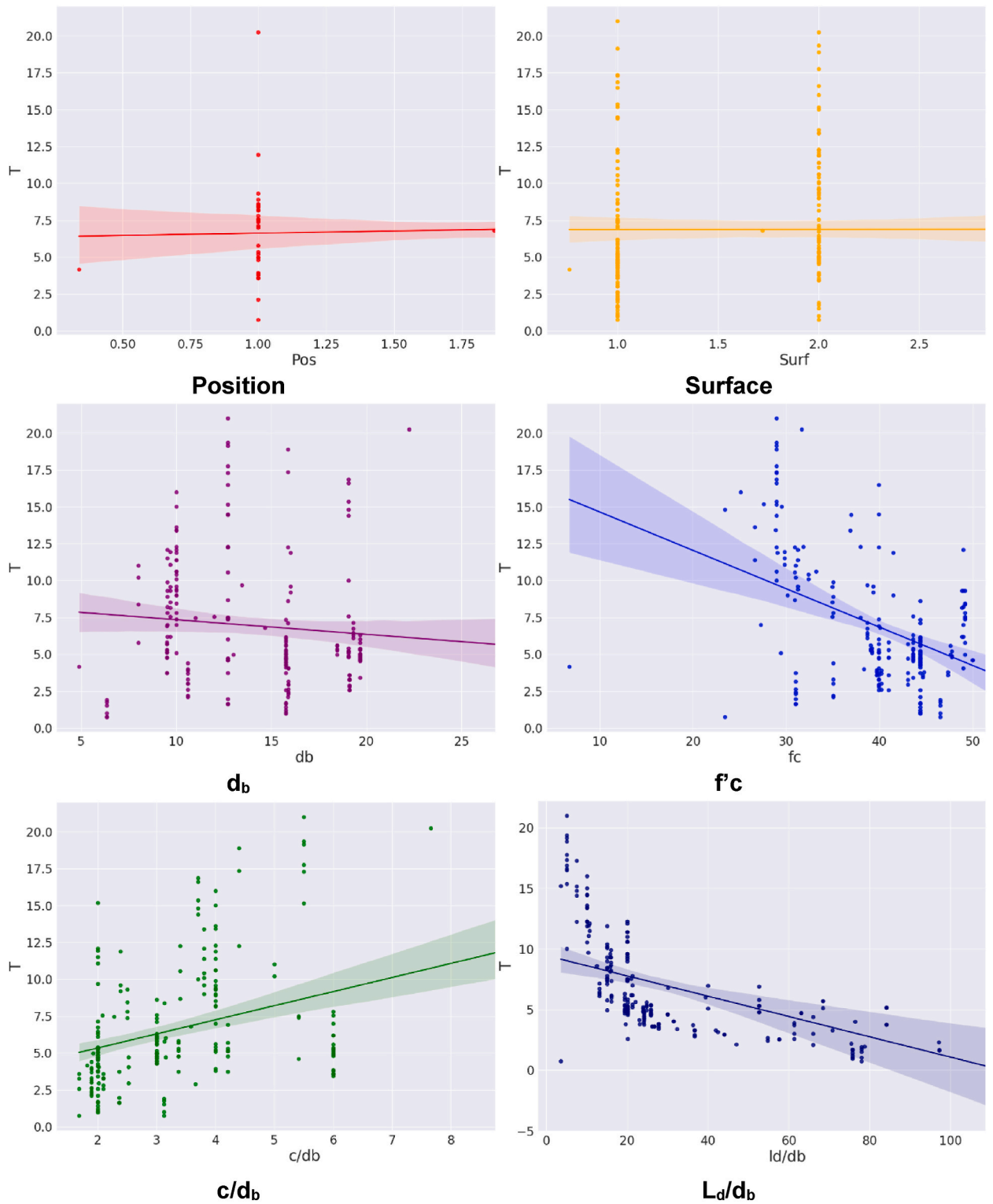
Fig. 4. Scatter plot for all the variables with bond strength (τ).

3.4. Statistical indicators

In this work the statistical measures, including the mean absolute error (MAE), root mean squared error (RMSE), mean, and co-efficient of determination (R^2), were employed in a comparative analysis to evaluate both new and existing analytical methods. These

Table 5

MOGA- EPR model equation.

FRP bars Predicted Bond strength ($\tau_{predicted}$) Equation	Equation #
$\tau_{predicted} = a_1 \times \sqrt{f_c'} + a_2 \times \sqrt{d_b} \times \sqrt{\dfrac{l_d}{d_b}} +$ $a_3 \times \sqrt{d_b} \times \sqrt{\dfrac{c}{d_b}} +$ $a_4 \times d_b \times \sqrt{f_c'} \times \dfrac{l_d}{d_b} +$ $a_5 \times \text{Pos} \times \sqrt{\text{Surf}} \times d_b \times \dfrac{l_d}{d_b} + a_6$	Eq. (11)
Coefficients: $a_1 = -2.786; a_2 = -1.2989; a_3 = 4.1285 \times 10^{-1}; a_4 = 2.8564 \times 10^{-3}$ $a_5 = 4.4543 \times 10^{-3}; a_6 = 37.7581$	

Table 6

Main configuration parameters and modifications of the GEP models.

GEP parameter	Setting parameters	
	Model (1)	Model (2)
Number of chromosomes	30	30
Head size	10	9
Number of genes	6	5
Function set	$+, -, \times$ and$/$	$+, -, \times, /$ and $\sqrt{}$
Fitness function	RMSE	RMSE
Mutation rate	0.00138	0.00138
Inversion rate	0.00546	0.00546
Gene recombination rate	0.00277	0.00277
Gene transposition rate	0.00277	0.00277
Random chromosomes	0.0026	0.0026

measures are commonly used in previous studies, such as those conducted by Ref. [48–52].

The MAE and RMSE values are utilized to assess the goodness of fit, where lower values indicate a more desirable fit. Ideally, the mean value should be 1.0, as higher values suggest an overall overestimation of the bond strength between FRP bars and concrete (τ), while lower values indicate an overall underestimation.

The equations provided (Equations (14)–(17)) involve variables, where n represents the number of data points considered in the evaluation. Additionally, τ_p and τ_e correspond to the predicted and experimental bond strength of FRP bars in concrete, respectively.

$$\text{MAE} = \frac{1}{n} \sum_{1}^{n} |\tau_p - \tau_e| \qquad \text{Eq. (14)}$$

$$\text{RMSE} = \sqrt{\frac{1}{n} \sum_{1}^{n} (\tau_p - \tau_e)^2} \qquad \text{Eq. (15)}$$

$$\text{Mean} = \frac{1}{n} \sum_{1}^{n} \left(\frac{\tau_p}{\tau_e} \right) \qquad \text{Eq. (16)}$$

$$R^2 = \left(\frac{\sum_{i=1}^{n} \left(\tau_p - \tau_{P_{average}} \right) \left(\tau_e - \tau_{e_{average}} \right)}{\sqrt{\sum_{i=1}^{n} \left(\tau_p - \tau_{P_{average}} \right)^2 \sum_{i=1}^{n} \left(\tau_e - \tau_{e_{average}} \right)^2}} \right)^2 \qquad \text{Eq. (17)}$$

4. Results

In this paper, the both evolutionary computation techniques GEP and MOGA-EPR are used to predict the Bond Strength (τ) of FRB reinforcement bars. The advantages of GEP include its versatility in handling various optimization problems, automatic generation of programs, flexibility in incorporating domain-specific knowledge, and effectiveness in capturing nonlinear relationships. However, it can endure from complexity, computational intensity, and premature convergence issues. On the other hand, MOGA-EPR offers advantages such as multi-objective optimization, robustness across different problem types, and adaptability to problem characteristics. Nonetheless, it also has drawbacks, including high computational costs, the need for parameter tuning, difficulties in interpreting trade-offs, and convergence to approximate solutions.

The statistical metrics that were derived for the training and testing datasets for the MOGA-EPR and GEP techniques are shown in

Table 7

GEP models equations.

Model #	Predicted Bond strength of FRP bars in concrete ($\tau_{\text{predicted}}$) Equation	Equation #
Model (1)		Eq. (12)

$$\tau_{\text{predicted}} = \frac{d_b}{\left(\left(\frac{l_d}{d_b} - \text{Pos}\right) \times \left((b_1 \times \text{Surf}) - \frac{c}{d_b}\right)\right) + \text{Pos}} + \frac{c}{d_b} - \frac{\left(f_c' \times \frac{c}{d_b}\right) + f_c' + \frac{l_d}{d_b}}{(b_2 - f_c') \times \frac{l_d}{d_b}} + \frac{b_3 \times \frac{c}{d_b}}{\frac{l_d}{d_b} \times \frac{\left(\frac{b_4}{d_b}\right) + \text{Pos}}{2\text{Surf}}} +$$

$$(b_5 \times b_6) + \frac{\frac{l_d}{d_b}}{\left(\frac{b_7 \times \text{Surf} \times f_c}{\text{Surf} + \frac{l_d}{d_b}}\right) \times (\text{Surf} + b_8) \times \left(\frac{c}{d_b} + d_b\right)} +$$

$$\frac{\frac{l_d}{d_b} + 2d_b + \text{Pos} + f_c' - \text{Surf}}{b_9}$$

Coefficients:

$b_1 = 7.996940321059$; $b_2 = 20.31748431911480$;
$b_3 = 4.41390901355883$; $b_4 = 8.82044040751257$;
$b_5 = -1.75009609211671$; $b_6 = -8.74386428073651$;
$b_7 = -3.48113667003565$; $b_8 = -3.27172224073646$;
$b_9 = -9.09850857868821$

Model #	Predicted Bond strength of FRP bars in concrete ($\tau_{\text{predicted}}$) Equation	Equation #
Model (2)	$\tau_{\text{predicted}} =$	Eq. (13)

$$\frac{\text{Pos} \times (d_b - c_1)}{c_2} + \frac{\text{Pos} \times \frac{l_d}{d_b}}{f_c} + \sqrt{\left(\left(\frac{c_3}{\frac{c}{d_b} \times c_4}\right) - \left(\frac{c_5}{f_c}\right) + \text{Surf}\right) \times c_6} +$$

$$\frac{\text{Pos} \times c_7 \times c_8}{\frac{l_d}{d_b} + \text{Pos} + \frac{\text{Surf}}{\frac{c}{d_b}}} + \text{Pos} + \frac{c_9}{\frac{c}{d_b} \times (d_b - c_{10})} + \frac{\frac{l_d}{d_b}}{c_{11}} + \sqrt{c_{12} + \sqrt{c_{13}}} - \left(\left(\left(\frac{c}{d_b} \times d_b\right) - c_{14}\right) \times \frac{c_{15}}{\frac{l_d}{d_b}}\right)$$

Coefficients:

$c_1 = -0.164072220822295$; $c_2 = -6.99535436508602$
$c_3 = -15.2727586376696$; $c_4 = 4.12355529746554$
$c_5 = -109.427008426539$; $c_6 = 6.64424787133396$
$c_7 = 9.85867884247271$; $c_8 = 3.48719039097061$
$c_9 = 3.8402287215582$; $c_{10} = 6.94130507230984$
$c_{11} = -11.2602538764556$; $c_{12} = -0.952185415136715$
$c_{13} = 8.36977943998535$; $c_{14} = -51.3418281307054$
$c_{15} = 8.40446223029267$; $c_{16} = -0.14901218674942$

Table 8

Evaluation of statistical accuracy for the developed models across both datasets.

Statistical indicators	Developed Models		
	MOGA-EPR Model	GEP Model (1)	GEP Model (2)
Training Dataset			
MAE (MPa)	0.97	0.94	0.93
RMSE (MPa)	1.28	1.24	1.26
Mean	1.05	1.00	1.01
R^2	0.91	0.92	0.91
Testing Dataset			
MAE (MPa)	0.84	0.73	0.79
RMSE (MPa)	1.13	0.87	1.07
Mean	1.18	1.08	1.01
R^2	0.91	0.94	0.94

Table 8. These measurements, which were used to forecast bond strength values and contrast them with the bond strength determined through testing, include mean absolute error (MAE), root mean squared error (RMSE), mean, and coefficient of determination (R^2).

According to the results shown in Table 8, the developed methods' MAE falls between 0.93 and 0.97 MPa for training datasets and 0.73 and 0.84 MPa for testing datasets. The training datasets produce RMSE scores between 1.24 and 1.28, meanwhile, the testing datasets produce RMSE ratings between 0.87 and 1.13 MPa. The training dataset's mean spans from 1.00 to 1.05, whereas the testing dataset's mean falls between 1.18 and 1.01. Last but not least, the R^2 values for the testing datasets range from 0.93 to 0.97 and from 0.91 to 0.94 for the training datasets.

The statistical metrics derived from the training and testing datasets and shown in Table 8 are positive and remarkably similar. In comparison to the two GEP models, the MOGA-EPR model has the highest R^2, with the GEP model (2) having a higher R^2 than the GEP

model (1). Additionally, MOGA-EPR has among the models the lowest MAE and RMSE values. For each model, the mean values are all somewhat near 1.

The predicted and experimental values for the training and testing datasets for the three models are compared in Figs. 5 and 6. The findings show that most predictions fall within a 20 % margin of error and are in line with the perfect fit line. This constancy suggests accurate forecasts.

5. Comparison with existing models

In this study, the bond strength of the FRP bars with concrete is estimated using GEP and MOGA-EPR methods. For comparison, 10 analytical equations were also assessed. The R^2, MAE, and RMSE for each of the models and references are shown in Table 9 and Fig. 7.

As shown in Table 9, The MAE values range from a low of 0.87 MPa (achieved by the GEP Model 2) to a high of 9.49 MPa (observed in the CEB-FIP model [36]). Similarly, the RMSE values span from 1.18 MPa (achieved by both GEP Model 1 and GEP Model 2) to 10.28 MPa (in the CEB-FIP model [36]). The mean values range from a low of 1.02 MPa (achieved by both GEP Model 1 and GEP Model 2) to a high of 3.49 MPa (in the CEB-FIP model [36]). Lastly, as shown in Table 9 and Fig. 7, the R^2 values vary between a high of 0.92
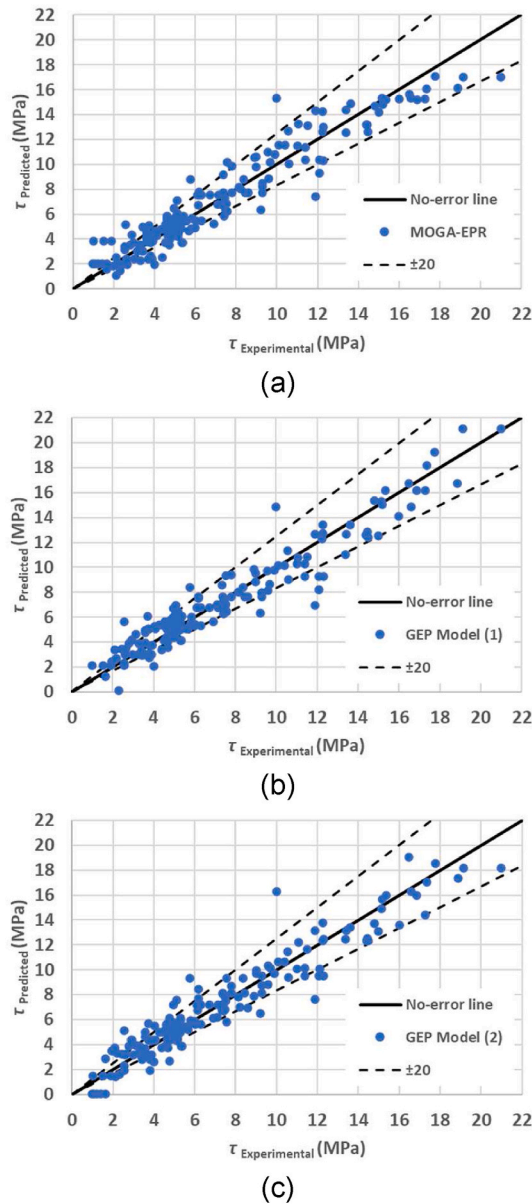

(a)

(b)

(c)

Fig. 5. Correlation between predicted and experimental bond strength utilizing the developed models for the training dataset: (a) MOGA-EPR, (b) GEP model (1), and (c) GEP model (2).
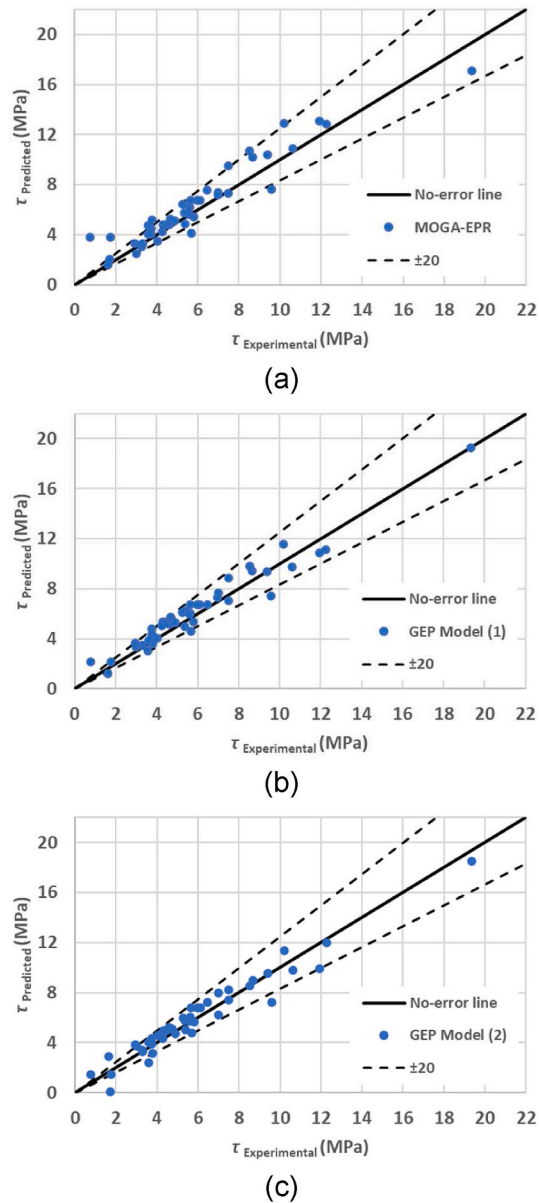
Fig. 6. Correlation between predicted and experimental bond strength utilizing the developed models for the testing dataset: (a) MOGA-EPR, (b) GEP model (1), and (c) GEP model (2).

(achieved by both GEP Model 1 and GEP Model 2) and a low of 0.23 (in the Wang et al. Model II [33]).

The comparison of statistical accuracy measures reveals MOGA-EPR demonstrates good performance across various statistical accuracy measures. It achieves a low MAE value of 0.94 MPa, indicating a small average difference between its predicted values and the actual values. Additionally, it has an RMSE value of 1.25 MPa, implying relatively accurate predictions. The mean value of 1.08 MPa suggests that its average predictions are close to the actual values. Moreover, MOGA-EPR achieves an R^2 value of 0.91, indicating a strong correlation and a good fit between its predicted values and the actual values. However, the GEP models (GEP Model (1) and GEP Model (2)) consistently outperform the other models across multiple measures. The GEP models achieve the lowest MAE values of 0.87 MPa and 0.90 MPa, and the lowest RMSE values of 1.18 MPa, indicating superior accuracy and precision in their predictions. Moreover, the GEP models exhibit the lowest mean values of 1.02 MPa, indicating their average predictions are closer to the actual values compared to other models. Additionally, the GEP models demonstrate the highest R^2 values of 0.92, indicating a stronger correlation and a better fit between their predicted values and the actual values. These findings highlight the GEP models' exceptional performance in terms of MAE, RMSE, mean, and R^2 compared to the other models.

The ranges illustrated in Table 9 and Fig. 7 show the diversity in performance among the models and highlight the superior accuracy and predictive capabilities of the GEP models compared to others in the comparison.

Table 9

Comparative analysis of statistical accuracy between the developed and existing models across all datasets.

Model	MAE (MPa)	RMSE (MPa)	Mean	R^2
MOGA-EPR	0.94	1.25	1.08	0.91
GEP Model (1)	0.90	1.18	1.02	0.92
GEP Model (2)	0.87	1.18	1.02	0.92
Wang et al. Model I, 2021 [33]	4.10	5.92	0.67	0.29
Wang et al. Model II, 2021 [33]	5.74	7.09	0.23	0.43
MGGP, 2019	0.95	1.25	1.05	0.91
Diab et al., 2014 [34]	5.96	6.59	2.41	0.73
Aslani & Nejadi, 2012 [35]	3.11	4.33	0.76	0.30
ACI, 2006	1.85	2.65	0.99	0.68
CEB-FIP I, 1993 [36]	9.49	10.28	3.49	0.31
CEB-FIP II, 1993[36]	3.07	4.59	1.09	0.32
CEB-FIP III, 1993 [36]	9.30	10.08	3.44	0.31
Orangun et al., 1977 [37]	3.02	4.03	1.46	0.21
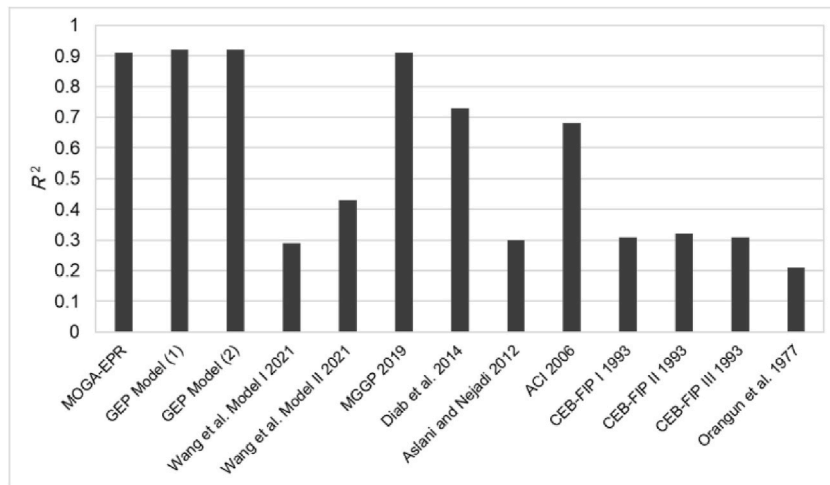
Fig. 7. Comparison between R^2 values for different developed and current models.

6. Sensitivity studies

After evaluating the strength of the bond between FRP bars and concrete using different models in the preceding above sections, the GEP model (1) was chosen for additional sensitivity analyses. The reason behind selecting the GEP model (1) is its simplicity, which allows for a straightforward examination of the impact of various parameters on bond strength. Through these analyses, the aim is to illustrate how the bond strength between FRP bars and concrete is influenced by modifying the values of input variables.

6.1. Compressive strength of concrete (f_c')

In this section, the effect of changing the compressive strength of concrete (f_c') to the bond strength values is studied for the top and bottom locations of the FRP bars and different types of surface characteristics.

Figs. 8 and 9 demonstrate that an increase in the compressive strength of concrete leads to a decrease in the bond strength (τ) of FRP reinforcement bars in concrete. Fig. 8 illustrates the impact of compressive strength on bond strength, specifically focusing on the top position of the FRP bars and displaying three different surface characteristics. It highlights the significant influence of surface characteristics on compressive strength. Similarly, Fig. 9 reveals consistent results for the bottom location of the FRP bars.

According to Nepomuceno et al. [8] from the literature review, the compressive strength of concrete is vital for the bond strength between FRP bars and concrete. The bond strength refers to the ability of the FRP bars to transfer stress to the surrounding concrete, ensuring effective load transfer and structural performance.

The interfacial shear stress between the FRP bars and concrete is influenced by the compressive strength of concrete, which provides a stiffer and stronger medium for stress transfer. The bond stress-slip relationship between FRP bars and concrete is also affected by the compressive strength of concrete.

Failure modes observed between FRP bars and concrete are related to the mechanical properties of concrete, including its compressive strength. Additionally, the long-term durability of the bond is influenced by the compressive strength of concrete [8].

Predictions for bond strength retention consider the effects of compressive strength when assessing the structural safety of FRP-reinforced concrete structures. While other factors such as fiber type, embedded length, bar diameter, and surface treatment also
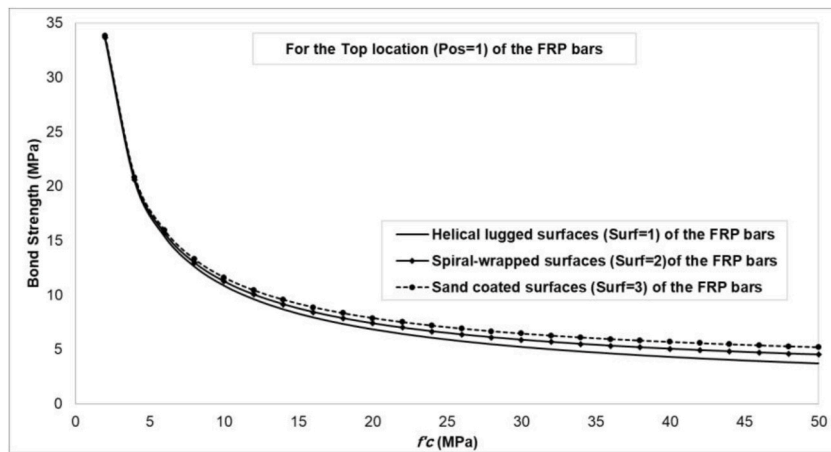
Fig. 8. Influence of Concrete Compressive Strength ($f'c$) on Bond Strength (τ) for Top placement of FRP Bars (Pos = 1) with varying surface properties.
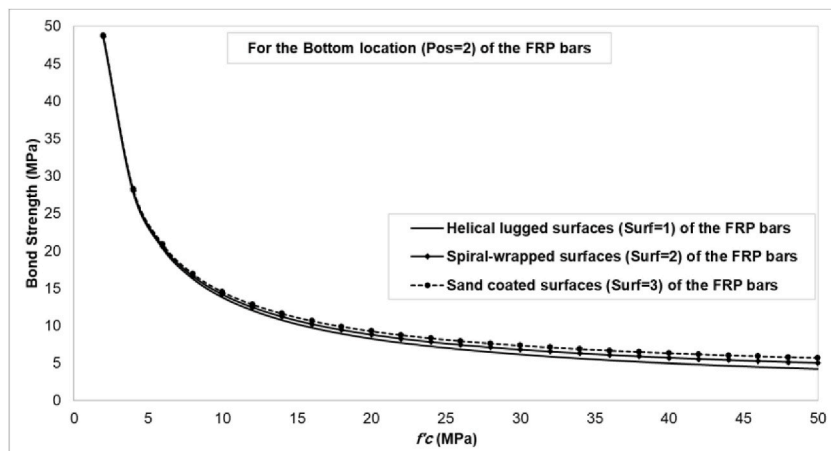

Fig. 9. Influence of Concrete Compressive Strength ($f'c$) on Bond Strength (τ) for Bottom placement of FRP Bars (Pos = 2) with varying surface properties.

influence the bond strength, the compressive strength of concrete plays a significant role [8].

6.2. The effect of position and surface

The developed models equations for predicting the bond strength of FRP bars in concrete include two input variables: surface characteristics of the bar (Surf) and the position of the bar (Pos). Despite the importance of these variables, none of the previously mentioned equations in Table 1 accounted for them due to the difficulty of incorporating them into practical equations.

Therefore, in this study, these two factors were excluded from the equation developed by the GEP model for bond strength prediction. After developing and analyzing various GEP models, the main setting parameters and adjustments adopted for the developed GEP model are presented in Table 10. The predicted equation for the bond strength of FRP bars in concrete (Equation (18)) is shown in

Table 10
Main configuration parameters and modifications of the GEP Model (3).

GEP parameter	Setting parameters
Number of chromosomes	30
Head size	8
Number of genes	4
Function set	$+, -, \times$ and$/$
Fitness function	RMSE
Mutation rate	0.00138
Inversion rate	0.00546
Gene recombination rate	0.00277
Gene transposition rate	0.00277
Random chromosomes	0.0026

Table 11
GEP Model (3) equation.

Model #	Predicted Bond strength of FRP bars in concrete ($\tau_{predicted}$) Equation	Equation #
Model (3)	$$\tau_{predicted} = \left(\left(\frac{d_1 \times \frac{c}{d_b}}{\frac{l_d}{d_b} \times (f_c' - d_2)} \right) \times \left(\frac{l_d}{d_b} + d_3 \right) \right) + \frac{\frac{l_d}{d_b} \times \frac{c}{d_b}^2}{\left(f_c - \frac{c}{d_b} \right) \times d_4} +$$ $$\frac{c}{d_b} + \left(d_5 \times \frac{l_d}{d_b} \right) - (d_6 \times f_c') + \frac{d_b}{d_7} - d_8 + \frac{d_9}{\left(\frac{\frac{l_d}{d_b} - d_{10}}{d_{11}} + \frac{\frac{c}{d_b}}{d_{12}} \right)}$$ **Coefficients:** $d_1 = 3.22376520110033$; $d_2 = 10.4274414972655$; $d_3 = 12.66688313032930$; $d_4 = -9.15052166008696$; $d_5 = 3.07490059422623$; $d_6 = 0.15342170650938$; $d_7 = -4.92014893337809$; $d_8 = -4.78541266693748$; $d_9 = -16.7907452540866$; $d_{10} = -2.0386997105469$; $d_{11} = -5.99729118911425$; $d_{12} = -6.47822496331328$	Eq. (18)

Table 11.

Table 12 displays the statistical accuracy analysis of the developed model using all the datasets. It reveals that the GEP model (3) achieves high accuracy, with an R^2 value of 0.91 and a mean value close to 1.

The significance of this developed equation lies in its ability to be utilized and compared with various existing models and equations that neglected the Surface and Position factors.

7. Conclusions

The results of this study demonstrate the accuracy and performance of the developed models for predicting the bond strength between FRP bars and concrete. In this work the input considered to predict the bond strength where the compressive strength of the concrete, the bar diameter, bar embedment length to bar diameter ratio, and concrete cover-to-bar diameter ratio, the bar position and surface type. To ensure accurate predictions, it is fundamental to develop prediction equations that consider the surface characteristics of the FRP bar and its position within the concrete. By incorporating these factors, engineers and designers can obtain more reliable estimations of the bond strength of FRP bars in concrete, thus ensuring reinforced concrete's structural integrity and safety.

Taking into consideration the limitation of this work the following conclusion can be drawn:

- The MOGA-EPR model and the GEP models display very good statistical indicators, including low MAE and RMSE values for both testing and training sets, close-to-1 Mean values for both testing and training sets, and high R^2 values between 0.91 and 0.94 for the testing set. The comparison of the predicted and experimental values further supports the reliability of the models.
- The GEP and MOGA-EPR models regularly outperform the other models in terms of MAE, RMSE, Mean, and R^2 when compared to already developed design code and the analytical equations. Improved accuracy, precision, and correlation with the actual values are all displayed by the GEP models.
- The GEP and MOGA-EPR models sensitivity studies emphasize that surface properties and position affect bond strength. These elements, which were overlooked, are included in the models, producing more precise predictions.

The results of this study assist in explaining how FRP-reinforced concrete structures behave and offer insightful information for structural design and analysis. The created models, especially the GEP models, provide accurate tools for estimating bond strength while considering various parameters.

These models show the importance of some of the disregarded parameters in design, such as the bar's position and the surface properties of each bar used. There are limited tests on the impact of using FRP bars, and since they are novel materials implemented in the design, more research needs to investigate their behavior. The results of this work can aid in decision-making and improve the performance and safety of FRP-reinforced concrete structures.

Ethical statement

The authors assert that the research was conducted in accordance with ethical standards.

CRediT authorship contribution statement

Rwayda Kh S. Al-Hamd: Writing – review & editing, Writing – original draft, Resources, Methodology, Formal analysis, Data

Table 12
Evaluation of statistical accuracy for the developed GEP Model (3) across both datasets.

Model	MAE (MPa)	RMSE (MPa)	Mean	R^2
GEP Model (3)	0.96	1.27	1.07	0.91

curation, Conceptualization. **Asad S. Albostami:** Writing – original draft, Methodology, Investigation, Formal analysis, Data curation. **Saif Alzabeebee:** Methodology, Formal analysis. **Baidaa Al-Bander:** Formal analysis, Validation, Writing – original draft.

Declaration of competing interest

The authors declare that they have no known competing financial interests or personal relationships that could have appeared to influence the work reported in this paper.

Data availability

All data available in the study.

Acknowledgements

References

[1] S. Solyom, G.L. Balázs, Bond of FRP bars with different surface characteristics, Construct. Build. Mater. 264 (2020), https://doi.org/10.1016/j.conbuildmat.2020.119839.
[2] E. Cosenza, G. Manfredi, R. Realfonzo, Behavior and modeling of bond of FRP rebars to concrete, J. Compos. Construct. 1 (2) (1997), https://doi.org/10.1061/(asce)1090-0268(1997)1:2(40).
[3] A.D. Edwards, P.J. Yannopoulos, Local bond-stress to slip relationships for hot rolled deformed bars and mild steel plain bars, J. Am. Concr. Inst. 76 (3) (1979), https://doi.org/10.14359/6952.
[4] E. Makitani, I. Irisawa, N. Nishiura, Investigation of Bond in Concrete Member with Fiber Reinforced Plastic Bars, American Concrete Institute, ACI Special Publication, 1993, https://doi.org/10.14359/3929. SP138.
[5] H. Mazaheripour, J.A.O. Barros, J.M. Sena-Cruz, M. Pepe, E. Martinelli, Experimental study on bond performance of GFRP bars in self-compacting steel fiber reinforced concrete, Compos. Struct. 95 (2013), https://doi.org/10.1016/j.compstruct.2012.07.009.
[6] R. Okelo, R.L. Yuan, Bond strength of fiber reinforced polymer rebars in normal strength concrete, J. Compos. Construct. 9 (3) (2005), https://doi.org/10.1061/(asce)1090-0268(2005)9:3(203).
[7] F. Yan, Z. Lin, D. Zhang, Z. Gao, M. Li, Experimental study on bond durability of glass fiber reinforced polymer bars in concrete exposed to harsh environmental agents: freeze-thaw cycles and alkaline-saline solution, Compos. B Eng. 116 (2017), https://doi.org/10.1016/j.compositesb.2016.10.083.
[8] E. Nepomuceno, J. Sena-Cruz, L. Correia, T. D'Antino, Review on the bond behavior and durability of FRP bars to concrete, Construct. Build. Mater. 287 (2021), https://doi.org/10.1016/j.conbuildmat.2021.123042.
[9] R. Li, L. Liu, M. Cheng, Estimating the bond strength of FRP bars using a hybrid machine learning model, Buildings 12 (10) (2022), https://doi.org/10.3390/buildings12101654.
[10] Z. Pei, Y. Wei, Prediction of the bond strength of FRP-to-concrete under direct tension by ACO-based ANFIS approach, Compos. Struct. 282 (2022), https://doi.org/10.1016/j.compstruct.2021.115070.
[11] S.F. Shahri, S.R. Mousavi, Predicting the bond resistance of glass fiber bars in hinged beams employing enhanced soft computing techniques, KSCE J. Civ. Eng. 27 (9) (2023) 3901–3911, https://doi.org/10.1007/s12205-023-0197-7.
[12] H. Jahangir, Z. Nikkhah, D.R. Eidgahee, M.R. Esfahani, Performance based review and fine-tuning of TRM-concrete bond strength existing models, J. Soft Comput. Civil Eng. 7 (1) (2023) 43–55, https://doi.org/10.22115/scce.2022.349483.1476.
[13] M.Z. Naser, An engineer's guide to eXplainable Artificial Intelligence and Interpretable Machine Learning: navigating causality, forced goodness, and the false perception of inference, Autom. ConStruct. (2021), https://doi.org/10.1016/j.autcon.2021.103821.
[14] A. Ahangar Asr, A. Faramarzi, A.A. Javadi, An evolutionary modelling approach to predicting stress-strain behaviour of saturated granular soils, Eng. Comput. (2018), https://doi.org/10.1108/EC-01-2018-0025.
[15] A. Ahangar-Asr, A.A. Javadi, A. Johari, Y. Chen, Lateral load bearing capacity modelling of piles in cohesive soils in undrained conditions: an intelligent evolutionary approach, Appl. Soft Comp. J. (2014), https://doi.org/10.1016/j.asoc.2014.07.027.
[16] S. Alzabeebee, D.N. Chapman, A. Faramarzi, Development of a novel model to estimate bedding factors to ensure the economic and robust design of rigid pipes under soil loads, Tunn. Undergr. Space Technol. (2018), https://doi.org/10.1016/j.tust.2017.11.009.
[17] S. Alzabeebee, D.N. Chapman, A. Faramarzi, Economical design of buried concrete pipes subjected to UK standard traffic loading, Proc. Inst. Civ. Eng.: Struct. Build. (2019), https://doi.org/10.1680/jstbu.17.00035.
[18] S. Alzabeebee, R.K.S. Al-Hamd, A. Nassr, M. Kareem, S. Keawsawasvong, Multiscale soft computing-based model of shear strength of steel fibre-reinforced concrete beams, Innov. Infrastruct. Solut. 8 (1) (2023), https://doi.org/10.1007/s41062-022-01028-y.
[19] S. Alzabeebee, R.K.S. Al-Hamd, A. Nassr, M. Kareem, S. Keawsawasvong, Multiscale soft computing-based model of shear strength of steel fibre-reinforced concrete beams, Innov. Infrastruct. Solut. 8 (1) (2023), https://doi.org/10.1007/s41062-022-01028-y.
[20] S. Alzabeebee, Dynamic response and design of a skirted strip foundation subjected to vertical vibration, Geomech. Eng. (2020), https://doi.org/10.12989/gae.2020.20.4.345.
[21] Z. Du, M.A. Shahin, H. El Naggar, Design of ram-compacted bearing base piling foundations by simple numerical modelling approach and artificial intelligence technique, Int. J. Geosynth. Ground Eng. (2021), https://doi.org/10.1007/s40891-021-00287-6.
[22] A. Nassr, M. Esmaeili-Falak, H. Katebi, A. Javadi, A new approach to modeling the behavior of frozen soils, Eng. Geol. (2018), https://doi.org/10.1016/j.enggeo.2018.09.018.
[23] A. Nassr, A. Javadi, A. Faramarzi, Developing constitutive models from EPR-based self-learning finite element analysis, Int. J. Numer. Anal. Methods GeoMech. (2018), https://doi.org/10.1002/nag.2747.
[24] M.A. Shams, M.A. Shahin, M.A. Ismail, Design of stiffened slab foundations on reactive soils using 3D numerical modeling, Int. J. GeoMech. (2020), https://doi.org/10.1061/(asce)gm.1943-5622.0001654.
[25] A.S. Albostami, R. Kh. S. Al-Hamd, S. Alzabeebee, Shear strength assessment of reinforced recycled aggregate concrete beams without stirrups using soft computing techniques, J. Build. Pathol. Rehabil. 8 (2) (2023) 98. https://doi.org/10.1007/s41024-023-00343-w.
[26] A.S. Albostami, R. Kh. S. Al-Hamd, S. Alzabeebee, Soft computing models for assessing bond performance of reinforcing bars in concrete at high temperatures, Innovative Infrastructure Solutions 8 (8) (2023) 218. https://doi.org/10.1007/s41062-023-01182-x.
[27] A.S. Albostami, R. Kh. S. Al-Hamd, S. Alzabeebee, A. Minto, S. Keawsawasvong, Application of soft computing in predicting the compressive strength of self-compacted concrete containing recyclable aggregate, Asian J. Civ. Eng. (2023). https://doi.org/10.1007/s42107-023-00767-2.
[28] R.K.S. Al Hamd, S. Alzabeebee, L.S. Cunningham, J. Gales, Bond behaviour of rebar in concrete at elevated temperatures: a soft computing approach, Fire Mater. (2022), https://doi.org/10.1002/fam.3123.
[29] J. Dai, T. Ueda, Y. Sato, Development of the nonlinear bond stress–slip model of fiber reinforced plastics sheet–concrete interfaces with a simple method, J. Compos. Construct. 9 (1) (2005) 52–62, https://doi.org/10.1061/(asce)1090-0268(2005)9:1(52).

[30] A. Khalifa, W.J. Gold, A. Nanni, A. Aziz, Contribution of Externally Bonded FRP to Shear Capacity of RC Flexural Members, J. Compos. Constr. 2 (4) (1998) 195–202.

[31] H. Saghi, S.E. Hirdaris, Application of gene expression programming model to present a new model for bond strength of fiber reinforced polymer and concrete, J. Civil Eng. Mater. Appl. 3 (1) (2020) 15–29, https://doi.org/10.22034/JCEMA.2020.212110.1012. Published by Pendar Pub.

[32] H. Bolandi, W. Banzhaf, N. Lajnef, K. Barri, A.H. Alavi, An intelligent model for the prediction of bond strength of FRP bars in concrete: a soft computing approach, Technologies 7 (2) (2019), https://doi.org/10.3390/technologies7020042.

[33] X. Wang, Y. Liu, H. Xin, Bond strength prediction of concrete-encased steel structures using hybrid machine learning method, Structures 32 (2021), https://doi.org/10.1016/j.istruc.2021.04.018.

[34] A.M. Diab, H.E. Elyamany, M.A. Hussein, H.M. Al Ashy, Bond behavior and assessment of design ultimate bond stress of normal and high strength concrete, Alex. Eng. J. 53 (2) (2014), https://doi.org/10.1016/j.aej.2014.03.012.

[35] F. Aslani, S. Nejadi, Bond behavior of reinforcement in conventional and self-compacting concrete, Adv. Struct. Eng. 15 (12) (2012), https://doi.org/10.1260/1369-4332.15.12.2033.

[36] CEB-FIP, CEB-FIP Model Code 1990: Design Code, 1993. Bulletin d'Information 213/214.

[37] C.O. Orangun, J.O. Jirsa, J.E. Breen, Reevaluation of test data on development length and splices, J. Am. Concr. Inst. 74 (3) (1977), https://doi.org/10.14359/10993.

[38] S. Alzabeebee, M.K. Dhahir, S. Keawsawasvong, Predictive model for the shear strength of concrete beams reinforced with longitudinal FRP bars soil structure interaction of resilient systems view project soils' geotechnical properties: estimation and evaluation view project, Struct. Eng. Mech. 84 (2) (2022) 143–154, https://doi.org/10.12989/sem.2022.84.2.000.

[39] S. Alzabeebee, S.A. Mohamad, R.K.S. Al-Hamd, Surrogate models to predict maximum dry unit weight, optimum moisture content and California bearing ratio form grain size distribution curve, Road Mater. Pavement Des. 23 (12) (2022) 2733–2750, https://doi.org/10.1080/14680629.2021.1995471.

[40] S. Alzabeebee, D.N. Chapman, Evolutionary computing to determine the skin friction capacity of piles embedded in clay and evaluation of the available analytical methods, Transport. Geotech. 24 (2020), https://doi.org/10.1016/j.trgeo.2020.100372.

[41] A.A. Zuhaira, R.K.S. Al-Hamd, S. Alzabeebee, L.S. Cunningham, Numerical investigation of skimming flow characteristics over non-uniform gabion-stepped spillways, Innov. Infrastruct. Solut. 6 (4) (2021), https://doi.org/10.1007/s41062-021-00579-w.

[42] O. Giustolisi, D.A. Savic, Advances in data-driven analyses and modelling using EPR-MOGA, J. Hydroinf. 11 (3–4) (2009) 225–236, https://doi.org/10.2166/hydro.2009.017.

[43] A. Aytek, Ö. Kişi, A genetic programming approach to suspended sediment modelling, J. Hydrol. 351 (3–4) (2008) 288–298, https://doi.org/10.1016/j.jhydrol.2007.12.005.

[44] R. Faradonbeh, D. Armaghani, M.Z. Abd Majid, M. Md Tahir, B. Ramesh Murlidhar, M. Monjezi, H.M. Wong, Prediction of ground vibration due to quarry blasting based on gene expression programming: a new model for peak particle velocity prediction, Int. J. Environ. Sci. Technol. 13 (6) (2016) 1453–1464, https://doi.org/10.1007/s13762-016-0979-2.

[45] C. Ferreira, Gene expression programming: a new adaptive algorithm for solving problems, Complex Syst. 13 (2) (2001) 87–129.

[46] A.H. Gandomi, A.H. Alavi, C. Ryan, Handbook of Genetic Programming Applications, Springer, 2015.

[47] J.R. Koza, Genetic Programming: on the Programming of Computers by Means of Natural Selection, vol. 33, MIT Press, Cambridge, MA, 1992.

[48] J. Tinoco, A. Alberto, P. da Venda, A. Gomes Correia, L. Lemos, A novel approach based on soft computing techniques for unconfined compression strength prediction of soil cement mixtures, Neural Comput. Appl. 32 (13) (2020) 8985–8991, https://doi.org/10.1007/s00521-019-04399-z.

[49] W. Zhang, R. Zhang, C. Wu, A.T.C. Goh, S. Lacasse, Z. Liu, H. Liu, State-of-the-art review of soft computing applications in underground excavations, Geosci. Front. 11 (4) (2020) 1095–1106, https://doi.org/10.1016/j.gsf.2019.12.003.

[50] C.-F. Huang, Q. Li, S.-C. Wu, Y. Liu, J.-Y. Li, Assessment of empirical equations of the compression index of muddy clay: sensitivity to geographic locality, Arabian J. Geosci. 12 (4) (2019), https://doi.org/10.1007/s12517-019-4276-5.

[51] I.S. Alkroosh, M. Bahadori, H. Nikraz, A. Bahadori, Regressive approach for predicting bearing capacity of bored piles from cone penetration test data, J. Rock Mech. Geotech. Eng. 7 (5) (2015) 584–592, https://doi.org/10.1016/j.jrmge.2015.06.011.

[52] A. Kordnaeij, F. Kalantary, B. Kordtabar, H. Mola-Abasi, Prediction of recompression index using GMDH-type neural network based on geotechnical soil properties, Soils Found. 55 (6) (2015) 1335–1345, https://doi.org/10.1016/j.sandf.2015.10.001.